Peptide-Labeled Quantum Dots for Imaging GPCRs in Whole Cells and as Single Molecules

Min Zhou,[†] Eri Nakatani,[†] Luisa S. Gronenberg,[†] Takahira Tokimoto,[†] Mary J. Wirth,[†] Victor J. Hruby,[†] Amber Roberts,[‡] Ronald M. Lynch,[‡] and Indraneel Ghosh*[,†]

Department of Chemistry and Department of Physiology, University of Arizona, Tucson, Arizona 85721. Received July 2, 2006; Revised Manuscript Received October 25, 2006

We report a robust and practical method for the preparation of water-soluble luminescent quantum dots (QDs) selectively coupled through an amine or thiol linkage to peptide ligands targeted to G-protein coupling receptors (GPCRs) and demonstrate their utility in whole-cell and single-molecule imaging. We utilized a low molecular weight (~1200 Da) diblock copolymer with acrylic acids as hydrophilic segments and amido-octyl side chains as hydrophobic segments for facile encapsulation of QDs (QD 595 and QD 514) in aqueous solutions. As proof of principle, these QDs were targeted to the human melanocortin receptor (hMCR) by chemoselectively coupling the polymer-coated QDs to either a hexapeptide analog of α-melanocyte stimulating hormone or to the highly potent MT-II ligand containing a unique amine. To label QDs with ligands lacking orthogonal amines, the diblock copolymers were readily modified with water-soluble trioxa-tridecanediamine to incorporate freely available amine functionalities. The amine-functionalized QDs underwent facile reaction with the bifunctional linker NHS−maleimide, allowing for covalent coupling to GPCR-targeted ligands modified with unique cysteines. We demonstrate the utility of these maleimide-functionalized QDs by covalent conjugation to a highly potent Deltorphin-II analog that allowed for selective cell-surface and single-molecule imaging of the human δ-opioid receptor (hDOR).

INTRODUCTION

Semiconductor nanocrystals, also called quantum dots (QDs), have received considerable attention due to their novel electronic and optical properties that are desirable for applications in biological imaging (*1*−*3*). Their broad absorption spectra, as well as their narrow and size-tunable emissions, by altering particle size, make it possible to excite all colors of QDs simultaneously with a single light source for multiplexing without substantial spectral overlap. The long photo luminescent lifetime of QDs (30−100 ns) also allow for imaging of living cells with minimal interference from background autofluorescence, while their resistance to photobleaching makes them useful for continuous monitoring of biological processes (*4*). These emerging probes can potentially aid in refining existing methods for drug targeting and in facilitating studies in basic biology (*5*, *6*).

Organometallic chemistry has provided synthetic pathways to robust, monodisperse, highly emissive nanomaterials, such as CdSe nanocrystals capped with ZnS shells. However, for biological imaging it remains challenging to choose appropriate organic coating agents to generate water-soluble QDs that maintain high luminescent quantum yields and stability. Ligand exchange is the most common method for generating water-soluble QDs; for example, simple thiol-containing molecules, such as mercaptoacetic acid, have been used to replace hydrophobic TOPO (trioctylphosphine oxide) coatings on the surface of CdSe/ZnS nanoparticles (*7*−*10*). In this case, the mercapto group thiolates the nanocrystal surface, while the carboxylic acid provides solubility. This method is simple, but the stability of the QDs in water is decreased (*11*) and the thiolation leads to eventual dissolution of the nanocrystals, resulting in the release of heavy atoms into solution (*12*). Phospholipid (*13*), polypeptide (*14*), bovine serum albumin (*15*), and silica (*12*) have also been used as capping agents but potentially lack simple and reliable methods for further bioconjugation to the targeting ligand for cell-surface imaging applications. Alternatively, amphiphilic di- and triblock copolymers for encapsulating QDs via a spontaneous self-assembly process (*16*, *17*) allow one to circumvent these potential drawbacks while maintaining the photoluminescent properties of the QD label. Besides generating water-soluble QDs, the conjugation of ligands to QDs is also critically important. Most reported methods for QD−ligand conjugation are achieved by precoupling the QDs with antibodies or streptavidin, followed by addition of hapten- or biotin-modified ligands. However, nonspecific interactions between the antibody or streptavidin with cell-surface targets are possible. Furthermore, both antibodies and streptavidin significantly increase the size of the QD complex (~50 nm), which could potentially affect accessibility to crowded cell-surface locations (*18*, *19*) and also interfere with receptor dynamics.

Though QDs are now commercially available, few robust literature methods have been reported for covalently conjugating peptide and peptidomimetic ligands to QDs. In a recent study, Schmidt and co-workers synthesized a small peptide ligand (RGD) with an added cysteine, which was directly used to coat bare quantum dot surfaces together with mercaptoacetic acid (*20*). However, the thiol coating may possibly lead to QD dissolution, as previously discussed. In more recent work, Rosenthal and co-workers coupled angiotensin II to carboxylic acid modified QDs by EDC (*21*). This method, though very useful, cannot be easily utilized when a ligand of interest contains two or more free amines and especially in instances

* Corresponding author. Indraneel Ghosh. E-mail: ghosh@email.arizona.edu. Department of Chemistry, The University of Arizona, P.O. Box 210041, 1306 E. University Blvd, Tucson, Arizona 85721-0041. Phone (520) 621-6331. Fax (520) 621-8407.

[†] Department of Chemistry.

[‡] Department of Physiology.

10.1021/bc0601929 CCC: $37.00
Published on Web 01/17/2007

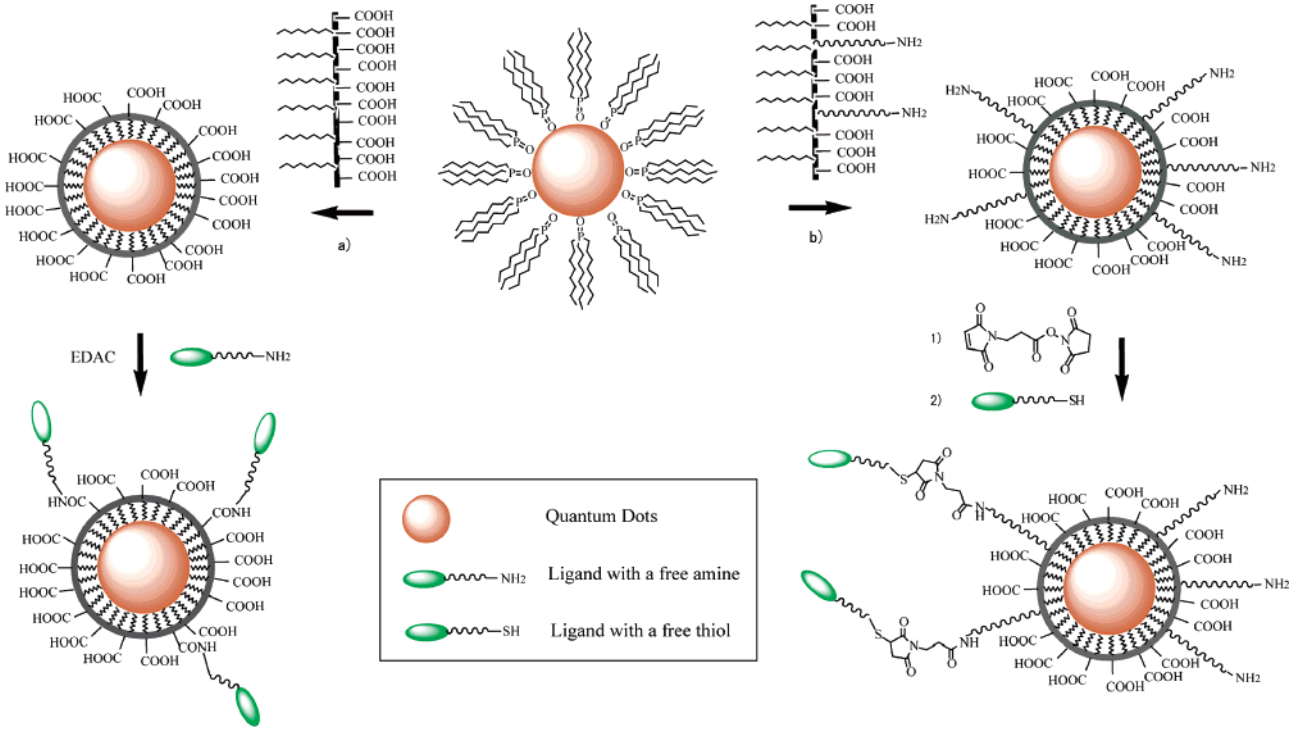

Figure 1. Synthesis of water-soluble QDs with associated ligand conjugation chemistry. (a) Carboxylic acid functionalized QDs for conjugation to ligands through EDAC coupling. (b) Amine-functionalized QDs for conjugation to thiol-containing ligands through bifunctional cross-linkers.

where the amines are important for bioactivity. Thus, it still remains challenging to optimize the chemistry as well as the process for generating water-soluble polymer-coated QDs that allow for facile covalent coupling to peptidic ligands that maintain their bioactivity.

Herein, we present a practical method for generating water-soluble QDs and the necessary chemistry for covalently coupling the QDs with G-protein couple receptor (GPCR) targeted ligands (Figure 1). GPCRs constitute a large and diverse family of proteins whose primary function is to transduce extracellular stimuli into intracellular signals. Since 50% of pharmaceuticals target GPCRs, new methods for imaging GPCRs at cell surfaces are of much interest. As proof of principle, we chose to target the QDs to the human melanocortin and δ-opioid receptors. We demonstrate the feasibility of QD514 conjugated to α-MSH analogs that effectively image melanocortin receptors overexpressed on HEK293 cells. We also demonstrate that QDs conjugated to Deltrophin-II analogs can be utilized for selectively imaging δ-opioid receptors on cell surfaces and for single-molecule imaging.

EXPERIMENTAL PROCEDURES

Instruments. QD absorbance was recorded by a Beckman DU520 instrument. Fluorescence spectra were recorded on a PTI fluorimeter (814 photomultiplier detection system and LPS-220B power supply). ^{1}H NMR spectra were recorded on a Bruker DRX-500 instrument.

General. All Fmoc-protected amino acids, BOP, HOBt, and Rink-amide resin used for peptide synthesis were purchased from Novabiochem. Boc-AEEEA (Boc-11-amino-3,6,9-trioxaundecanoic acid) was purchased from Peptides International. Bare QDs were synthesized using published methods (*22*) or purchased from Evident Technology. All other chemicals were purchased from Aldrich. Peptides were purified by reverse-phase HPLC (Varian) using a C18 column (Vydac.)

Synthesis of Octylamine-Modified Poyacrylic Acid (OPA). *A.* 10 mL of a poly(acrylic acid) sodium salt solution (MW ~1200, 45 wt % in water) was acidified by 5 mL of 12 N HCl, followed by addition of 200 mL of acetone under stirring to precipitate NaCl. After filtration, the acetone was removed from the filtrate by vacuum. The crude product was redissolved with 20 mL of water, frozen, and lyophilized. 4.5 g of white poly(acrylic acid) solid was collected.

B. 2.16 g of poly(acrylic acid) solid (0.03 mol of carboxylic acid) and 2.85 g of 1-ethyl-3-(3-dimethylaminopropyl)carbodiimide hydrochloride (EDAC, 0.015 mol) were transferred into a 100 mL round-bottom flask. 20 mL of DMF was added to dissolve the mixture. About 1.6 mL of octylamine (0.0096 mol) was added dropwise into the reaction flask. The clear solution was stirred overnight under argon. TLC (CH_2Cl_2/CH_3OH = 7:1, $R_{f(\text{octylamine})}$ = 0.55, $R_{f(\text{product})}$ = 0.24) was used to monitor the reaction. When the reaction was complete, DMF was removed by vacuum, and the residue was mixed with 10 mL of acetone and transferred into a centrifuge tube. 25 mL of water was added, and the gummy precipitated product was separated by centrifugation (3000 rpm for 5 min) and washed with water (25 mL × 3). The solid product was dissolved in 40 mL of ethyl acetate (gentle heating 40−50 °C was applied), and a tetramethylammonium hydroxide (6.4 g in 25 mL water) solution was added to the polymer solution and stirred for 10 min, before being transferred into a separation funnel. The yellowish aqueous layer was isolated in a centrifugation tube and acidified by 1 N HCl to pH 2. The precipitate was separated by centrifugation and washed with H_2O (15 mL × 2). The sticky solid was redissolved in ethanol, at which point the ethanol was removed under vacuum and 1.63 g of the yellow solid OPA was collected (45 ± 5% of the carboxylic acids were converted to octyl amide). ^{1}H NMR (*d*-CH_3OH): δ 0.85−0.92 (m, 3H), 1.20−1.35 (m, 10H), 1.40−1.55 (m, 2H), 1.55−1.95 (m, 3.2H), 2.05−2.50 (m, 2.4H), 2.95−3.28 (m, 2H).

Synthesis of Amine-PEG-Modified Polymer (APOPA). *A. Synthesis of Mono-Boc-Protected 4,7,10-trioxatridecanediamine.* 80 g of 4,7,10-trioxatridicanediamine (0.364 mol) was dissolved in 250 mL dichloromethane in a 500 mL round-bottom flask. 3.2 g of *t*-Boc anhydride (0.0147 mol) was dissolved in 20 mL of dichloromethane and added dropwise to the diamine solution

Scheme 1. Processing QDs with Water-Soluble Amphiphilic Shells

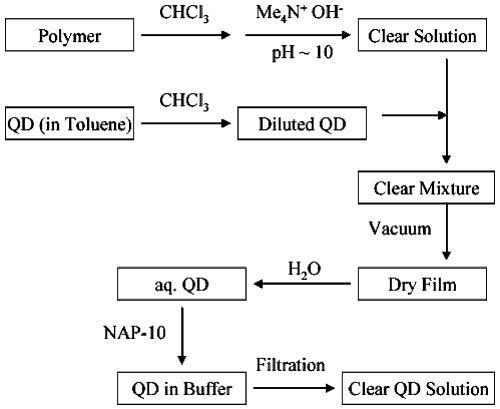

over 4 h with stirring. After the addition, the solution was stirred overnight. The solution was reduced to 150 mL under vacuum and extracted with water (300 mL × 6) to remove excess diamine. The organic layer was dried over Na_2SO_4, and the dichloromethane was removed under vacuum. About 2.54 g of mono-Boc-protected 4,7,10-trioxatridicanediamine (oily precipitate) was collected (yield 54%). ^{1}H NMR ($CDCl_3$): δ 1.45 (s, 9H), 1.74 (m, 4H), 2.80 (t, 2H), 3.22 (m, 2H), 3.52−3.67 (m, 12H).

B. Synthesis of Amine-PEG-Modified Triblock Copolymer. 383 mg of the octylamine-modified poly(acrylic acid) (OPA, ~0.2 mmol) and 190 mg of EDAC (1 mmol) were dissolved in 6 mL DMF in a 25 mL round-bottom flask, and the solution was stirred for 10 min. 128 mg of mono-Boc-protected 4,7,-10-trioxatridecanediamine (0.4 mmol) dissolved in 1 mL DMF was added into the reaction flask. The solution was stirred overnight, and the Kaiser test (*23*) was used to monitor the reaction. When the Kaiser test indicated no free amine in solution, DMF was removed by vacuum and the residue was transferred into a centrifuge tube, which contained 20 mL of H_2O. The precipitated product was isolated by centrifugation (3500 rpm for 8 min) and washed with 5 mL of H_2O. The product was redissolved in 3 mL of ethanol, which was subsequently removed by vacuum. 8 mL of 50% TFA in dichloromethane was added to the container to dissolve the residue and remove the Boc group. After a short reaction time, the solvent was removed by vacuum. The crude oily product was redissolved with 2 mL of ethyl acetate, and the solution was added dropwise into a centrifuge tube, which contained 30 mL of cold ether. The solid product was separated by centrifugation (3500 rpm for 5 min) and washed with 20 mL of ether. After drying, 120 mg of yellowish solid APOPA was obtained (12−14% of carboxylic acids were converted to amide-PEG-amine). ^{1}H NMR ($CDCl_3$): δ 0.80−0.95 (m, 3H), 1.02−1.39 (m, 10H), 1.39−1.60 (m, 2H), 1.60−2.15 (m, 3.1H), 2.15−2.55 (m, 1.4H), 2.78−3.00 (m, 1.1H), 3.0−3.4 (m, 2.9H), 3.5−3.88 (m, 3.3H).

Process for Coating QD with Amphiphilic Polymer Shell (Scheme 1). 50 mg of the OPA was dissolved in 4 mL of dichloromethane. Tetramethylammonium hydroxide (25 wt % in methanol) was used to adjust pH to 10. 500 μL of 0.12 mM bare QD514 in toluene (λ_{em} = 514 nm, Evident) were added to the solution and stirred for several minutes, at which time the solvent was removed under vacuum. The solid was redissolved in 500 μL of water and loaded onto a NAP-10 column (Amersham Biosciences). Phosphate buffer A (10 mM, pH 7.35) was used to elute the QDs. Fluorescent fractions were combined (~2 mL) and further filtered through a 0.45 μm Acrodisc syringe filter. The filtrate was dialyzed overnight in a Slide-A-Lyzer dialysis cassette (MWCO 7000, Pierce) against 400 mL of buffer A. The final aqueous QD stock solution was stored at 4 °C. QD concentration was determined by the absorption at 496 nm (ϵ = 50 000 M^{-1} cm^{-1}) based on the first excitation state of QD514.

The same process was repeated for coating QD595 (λ_{em} = 595 nm) with OPA. Twice the amount of OPA (100 mg) was used because of the larger size of QD595 (5 nm) compared to QD514 (3.2 nm). After dialysis, 2 mL of OPA-coated QD595 was collected. (Concentrations were determined by absorbance at 586 nm, based on the first excitation state of QD595 (ϵ = 400 000 M^{-1} cm^{-1}). Primary amine modified QD514 and QD595 were prepared using a similar protocol (Scheme 1), but starting with the amine-PEG-modified polymer, APOPA.

Peptide Synthesis and Purification. All ligands (NDP, MT-II, Deltorphin-II (Ile−Ile), and CCK; see Figure 2) were synthesized by solid-phase peptide synthesis using a standard fluorenylmethoxycarbonyl (Fmoc) strategy starting with Rink amide resin (*24*). The cyclization reaction of MT-II was performed according to the method reported by Hruby et al. (*25*) in 2002. Boc-AEEEA (PEG linker) was coupled at the N-terminal of norleucine before deprotection of glutamic acid and lysine, followed by cyclization.

The final peptides were cleaved from the resin and all protecting groups were removed by cleavage cocktail (100 mg of peptide resin was treated with 1 mL of cocktail) composed of TFA and scavengers (81.5% TFA, 5% H_2O, 5% thioanisole, 5% phenol, 2.5% ethanedithiol, and 1% triisopropylsilane) for 4 h at room temperature. The solution was filtered and precipitated by transferring into a centrifuge tube containing precooled ether. After centrifugation and 3× washes with fresh ether, the white solid was collected and lyophilized to yield crude product. The crude peptides were purified by reverse-phase HPLC (Varian) using a C18 column (Vydac). Peptides were purified with a linear gradient of 20% to 80% acetonitrile containing 0.1% TFA at a flow rate of 8 mL/min, for 50 min. The purified peptides were reinjected on reverse-phase HPLC and found to be >95% pure. The k' value of each product was determined by a C18 column with a linear gradient of 20% to 80% actonitrile containing 0.1% TFA at a flow rate of 1 mL/min for 20 min.

AEEEA-Nle-Glu-His-(D)Phe-Arg-Trp-NH$_2$ (NDP α-MSH Analogue). Mass spectroscopy (ESI): observed 886.5 (calculated 886.5). k' = 0.64.

MT-II (α-MSH Analogue). Mass spectroscopy (ESI): observed 1171.5 (calculated 1171.6). k' = 0.84.

Tyr-(D)Ala-Phe-Glu-Ile-Ile-Gly−Gly-(PEG)$_2$-Cys-Gly-NH$_2$ (Deltorphin II Analogue). Mass spectroscopy (ESI): observed 1345.5 (calculated 1346.8). k' = 0.95.

AEEEA-Asp-Tyr-N-MeNle-Gly-Trp-N-MeNle-Asp-Phe-NH$_2$ (CCK−B Ligand). Mass spectroscopy (ESI): observed 1244.3 (calculated 1244.8). k' = 1.50.

Preparation of NDP−QD514. 1.1 mL of 5 μM OPA-coated QD514 (5.5 nmol) was mixed with 10 μL of EDAC solution (0.05 mg/μl) and stirred for 10 min. 170 μL of 6.4 mM NDP-α-MSH stock solution (concentration was determined by absorption at 280 nm in 8 M guanidine) was added to the coated QD514 solution with stirring. The pH was adjusted to 7−8 with 25% tetramethylammonium hydroxide in methanol, and the Kaiser test was used to monitor reaction progress. After 6 h, the Kaiser test showed no free amine in solution, and the solution was loaded on a NAP-10 column and eluted with buffer A. The fluorescent fractions (~1.5 mL) were collected and dialyzed in a MWCO 3500 dialysis cassette against 500 mL of buffer A. After 10 h, fresh buffer was used for another 10 h dialysis. The final NDP−QD514 conjugate solution was 3 μM as determined by the absorption at 496 nm, described above.

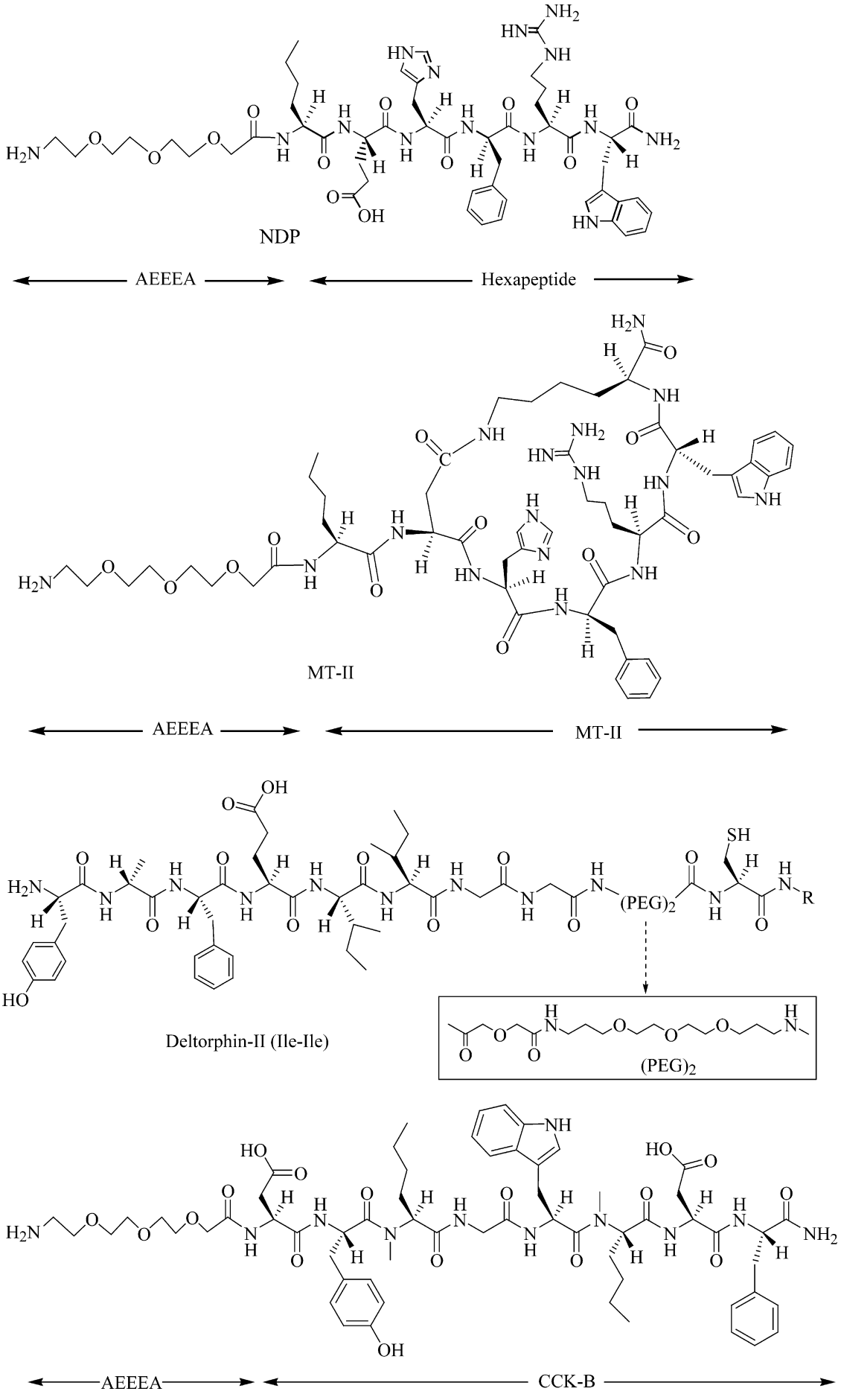

Figure 2. Structures of the GPCR-targeting ligands investigated.

Preparation of MT-II−QD595 and MT-II−QD514. 500 μL of 1.1 μM OPA-coated QD595 (0.55 nmol) was mixed with 20 μL of 2.8 mM MT-II (56 nmol) solution (concentration was determined by absorption at 280 nm in 8 M guanidine) in 80 μL of 0.1 M pH 9.2 sodium bicarbonate buffer. Under stirring, 20 μL of EDAC solution (40 mM) was added, and another 20 μL was added after 2 h. The Kaiser test was used to monitor the reaction. When the reaction was over (4−6 h), the solution was filtered with a 0.45 μm Acrodisc followed by dialysis in a MWCO 10 000 dialysis cassette against 400 mL × 2 of buffer A. Finally, ∼1.7 mL of 0.2 μM of the MT-II−QD595 conjugate solution was collected in which the ratio of MT-II to QD595 is about 100:1. The same procedure was used to conjugate MT-II to OPA-coated QD514.

Preparation of Deltorphin-II−QD595 and Deltorphin-II−QD514. 2.5 mg of *N*-(β-maleimidopropyloxyl)succinimide ester was dissolved in 1 mL DMSO to obtain a 10 mM cross-linker stock solution. 0.6 mg Deltorphin-II (Ile−Ile) was dissolved in 200 μL H_2O to obtain a 2 mM δ-opioid ligand stock solution (concentration was determined by the DTNB test based on the free thiol concentration (*26*)). 120 μL of APOPA-coated QD595 (2.8 μM, 0.33 nmol) was mixed with 10 μL of the cross-linker stock solution and incubated at room temperature for 1 h. The resultant clear solution was loaded on a NAP-10 column and eluted with buffer A. Fluorescent fractions (∼250 μL) were collected and mixed with 8 μL of the Deltorphin-II (Ile−Ile) stock solution (16 nmol) and 42 μL of buffer A. The mixture was equilibrated at room temperature for 1 h, at which time 3 μL of 100 mM β-mercaptoethanol was added to quench the unreacted maleimide. After 30 min, the reaction solution was filtered through a 0.45 μM Acrodisc and dialyzed in a MWCO 10 000 dialysis cassette against 400 mL × 2 of buffer A. The final 0.75 μM Deltorphin-II−QD595 solution was collected in which the maximal ratio of ligand/QD is about 50:1. A similar procedure was used to conjugate Deltorphin-II to APOPA-coated QD514. All QD or QD−ligand conjugate concentrations were determined as described above.

Immunocytochemistry. Cells grown on 25 mm round #1 coverslips were fixed with 3% paraformaldehyde, rinsed with 25 mM glycine, and permeabilized with 0.1% Triton X-100. The cells were incubated with the primary antibodies (rabbit polyclonal) against the δ-opioid receptor (Neuromics, Northfield, MN) or MC4R (RDI, Flanders, NJ) for 1 h at 25 °C. Cells were washed three times (5 min each) in phosphate buffered saline to remove unbound primary antibody. Since the MC4R antibody recognized an epitope on the cell exterior, live cells also were incubated with this antibody (10 μg/mL) for 5 min, washed in antibody-free buffer (2×, 5 min each), then fixed for subsequent processing. At this point, all fixed and permeabilized cells were incubated with secondary anti-rabbit IgG labeled with either Cy5 (Jackson ImmunoResearch) or FITC (Sigma) for 45 min at 25 °C. After washing, coverslips were mounted onto glass slides using a 50% glycerol/saline solution containing the antibleach agent paraphenylendiamine (0.1%). NDP−QD514 and Deltorphin-II(Ile−Ile)−QD595 were used for imaging MC4R or δ-opioid receptors as described in the results and discussion section.

For standard wide-field imaging, slides were mounted on the stage of an Olympus IX-70 microscope equipped with a 60 × 1.4 NA objective. Illumination was provided by a 100 W Hg lamp, and images were acquired using a liquid-cooled CCD camera (Roper Scientific) equipped with a Kodak CCD array (KAF1401E).

Single-Molecule Imaging: Incorporation of hDOR in Lipid Bilayer. The lipid bilayer was formed on a fused silica coverslip surface covered by a thin polyacrylamide film. It is possible to make a polymer brush of controlled thickness by the surface-initiated atom transfer radical polymerization (ATRP) (*27*, *28*). A 5-nm-thick polyacrylamide brush was prepared on the coverslip according to the same procedure previously reported (*29*). The lipid bilayer of 1-palmitoyl-2-oleoyl-*sn*-glycero-3-phosphocholine (POPC) with cholesterol (0−10%) was formed on the polyacrylamide-modified coverslip surface using a standard vesicle fusion procedure (*29*, *30*). The isolation and purification procedure of hDOR was as described previously (*29*, *31*). The receptor has a His tag and myc epitope on its C terminus, and is solubilized in buffered 1% dodecyl-β-D-maltoside solution. The hDOR solution was added into the buffer on the lipid membrane described above. This dilution of hDOR suspension allowed hDOR to be incorporated into the lipid bilayer. The lipid membrane was rinsed multiple times, then 50 mM phosphate buffer (0.5 M NaCl, pH 7.5) was added.

Single-Molecule Fluorescence Imaging. Single-molecule fluorescence imaging of the ligand binding was achieved by using a highly sensitive CCD camera coupled to an argon ion laser as an excitation source. The microscope (TE2000-U, Nikon) was designed for total internal reflection fluorescence imaging. For the excitation of the QDs, the blue line of the argon ion laser (488 nm, 0.05 mW) was used. The green line (514.5 nm, 0.26 mW) was used for Cy3 excitation. The laser beam was used to irradiate the sample in a total internal reflection mode via an oil-immersion 100× TIRF objective (NA 1.4, Nikon). A high-sensitivity CCD camera, PhotonMAX (512 × 512 pixels, Princeton Instruments), was used to detect emitted fluorescence from the QDs or Cy3 dye after reduction of stray light by the emission filter (595AF60, Omega Optical). The fluorescence image was captured as a 500 frame movie, in which the exposure (integration) time was 3 s for each frame.

RESULTS AND DISCUSSION

Design and Syntheses of Polymer-Coated QDs. For facile encapsulation of QDs, we chose to synthesize amphiphilic diblock (OPA) and triblock (APOPA) copolymers that would potentially impart solubility to the QDs in aqueous systems for biological imaging. In order to synthesize the block copolymers, we chose three different commercially available poly(acrylic acid) polymers with average molecular weights of 1200, 8000, and 100 000. For each polymer, 40% of the free acids were transformed to the hydrophobic octylamide groups such that the octyl chains would encapsulate and stabilize the QD while the unmodified carboxylic acids would provide solubility in an aqueous environment. The red QD 595 and green QD 514 were both coated with the amphiphilic diblock polymers in dichloromethane and were subsequently purified by size exclusion chromatography (NAP-10 column) followed by dialysis (Scheme 1). Nie and co-workers have recently utilized a similar strategy utilizing octylamine-modified triblock copolymer (MW 100 000, 25% of the free carboxylic acid was derivatized) as the QD coating polymer. All three copolymers afforded soluble QDs. Notably, the low molecular weight diblock polymer (MW 1200) provided the most reproducible coating for both the green and red QDs, where the copolymer contains ∼16 acid units of which 40% are modified with octylamine as evidenced by NMR. Both green and red QDs coated with this low molecular weight polymer were water-soluble and maintained high luminescence in aqueous solution. The absorption and emission spectra are very similar compared with those of TOPO-coated commercial QDs in toluene (Figure 3). We investigated whether these coatings provide extended stability and observed no changes in solubility or fluorescence over a 6 month period (stored at 4 °C). We also tested whether these coatings are stable to various pHs that may be found in different cellular environments and are also required in bioconjugation chemistries. We found that the QDs are stable between pH 3.5 and pH 10.5. Thus, our

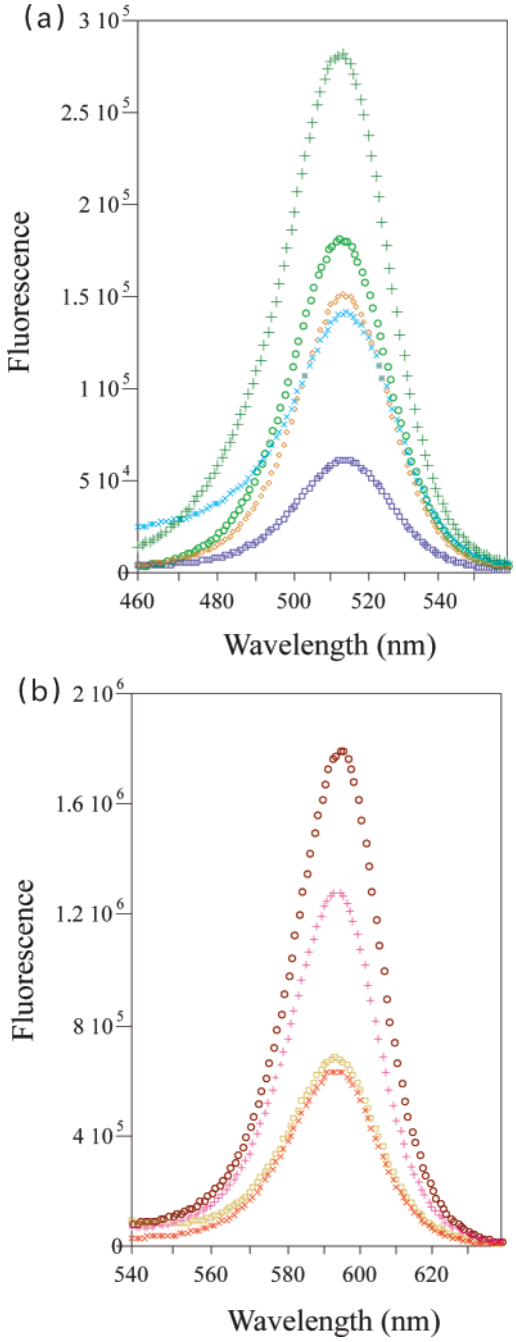

Figure 3. Photoluminescence of uncoated QDs and their GPCR−ligand conjugates. (All samples are normalized to 1 μM of QD) (a) QD514 labeled ligands (green ○, Evidot QD514; red ◇, NDP−QD514; blue □, MT-II−QD514; cyan ×, Deltorphin-II(Ile−Ile); green +, CCK-B−QD514). (b) QD595 labeled ligands. (dark red ○, Evidot QD595; yellow □, MT-II−QD595; red ×, Deltorphin-II(Ile−Ile); magenta +, CCK-B−QD595).

results provide a robust method for synthesizing stable water-soluble QDs suitable for covalent labeling with any macromolecule containing free amines via EDAC-mediated amide bond formation.

In many peptide ligands, the amino terminal and/or free amines play an important role in ligand/receptor interactions. For such ligands, the EDAC-mediated coupling to carboxylic acid functionalized QDs is not feasible. Thus, we also synthesized amino functionality containing amphiphilic copolymers as an alternate QD coating that can be further modified with standard NHS containing bifunctional cross-linkers. We chose to functionalize the 40% octylamine modified poly(acrylic acid) (OPA) with 4,7,10-trioxatridecanediamine. We protected one of the amines with *t*-Boc, while the free amine was coupled to the polymer using EDAC followed by deprotection of *t*-BOC with TFA to give the amino-modified OPA. ^{1}H NMR showed that each polymer chain contained an average of six octyl chains and two free amines. The new amino-amphiphilic polymer (APOPA) was utilized to successfully encapsulate the QDs utilizing the same protocol described for the diblock copolymer (OPA) (Scheme 1). The properties of these amine-functionalized APOPA-coated QDs were found to be very similar to the OPA-coated QDs, with excellent water solubility, stability, and luminescent properties. With both types of water-soluble QDs in hand, we turned to applying them for ligand conjugation for biological imaging.

Bioconjugation of Ligands to QDs for GPCR Imaging. In order to showcase our bioconjugation chemistries and provide useful biological reagents, we chose to target two different G-protein-coupled receptors (GPCRs), the human melanocortin receptor (hMCR) and the human δ-opioid receptor (hDOR). Cell-surface receptors, particularly GPCRs, play a central role in cellular signaling and are important targets for modern pharmaceuticals (*32*). Hence, there is a continuing demand for reliable methods to directly probe cellular localization, receptor density, and trafficking. As such, we chose ligands with high affinity for the chosen GPCRs to allow for imaging with the QD label. For hMCR targeting, we utilized two analogues of α-melanocyte-simulating hormone (α-MSH), NDP and MT-II, developed by Hruby and co-workers (*33*, *34*). NDP and MT-II (Figure 2) ligands were synthesized by standard solid-phase peptide synthesis and purified. The purified peptides were directly conjugated to the OPA copolymer coated QD514 and QD595 by utilizing the water-soluble EDAC-coupling reagent. The carboxylic acids on the QD surface were activated with EDAC followed by addition of the amine-containing ligands to generate the QD−α-MSH conjugate (Figure 1, route a). We also synthesized another potent ligand, Asp-Tyr-*N*-MeNle-Gly-Trp-*N*-MeNle-Asp-Phe-NH_2 (CCK−B), which has been shown to be a selective CCK−B-type analogue with an IC_{50} of 0.13 nM (*35*) and conjugated this ligand to our soluble QDs using the above-described methodology to yield CCK−B−QD514 and CCK−B−QD595.

In an effort to provide a general strategy for QD conjugation, we also considered the possibility that many peptide ligands could contain two or more free amines and thus not allow for selective conjugation to QDs. Alternatively, the N-terminal amine in the ligand could be important for biological activity, which would preclude the EDAC-mediated coupling reaction described above. Considering this situation, we prepared QDs coated with amine functionalities (APOPA) that could be modified by a suitable bifunctional linker, where one end provides an activated ester that can react with a free amine on the QD surface while the other end provides a maleimide that can specifically react with a unique thiol that is engineered into a ligand. To demonstrate the feasibility of this approach, we synthesized a highly potent Deltorphin-II analog, Tyr-(D)Ala-Phe-Glu-Ile-Ile-Gly (Deltorphin-II(Ile−Ile)), developed by Sasaki (*36*) to selectively target the δ-opioid receptor (K_d = 67 pM). We incorporated a short linker and a cysteine at the C-terminus of this ligand for facile conjugation at pH 6−8 to the maleimide-functionalized amine-bearing QDs (Figure 1, route b). The peptide was conjugated to the QDs to yield Deltorphin-II(Ile−Ile)−QD514 and Deltorphin-II−QD595.

Having all of the four different sets of GPCR ligand−QD conjugates in hand, we compared them to the commercial QDs in toluene. All the water-soluble ligand-modified QDs were shown to maintain high photoluminescence in aqueous conditions (Figure 3). NDP−QD514 and Deltorphin-II(Ile−Ile)−QD514 almost have the same fluorescence intensity as the bare

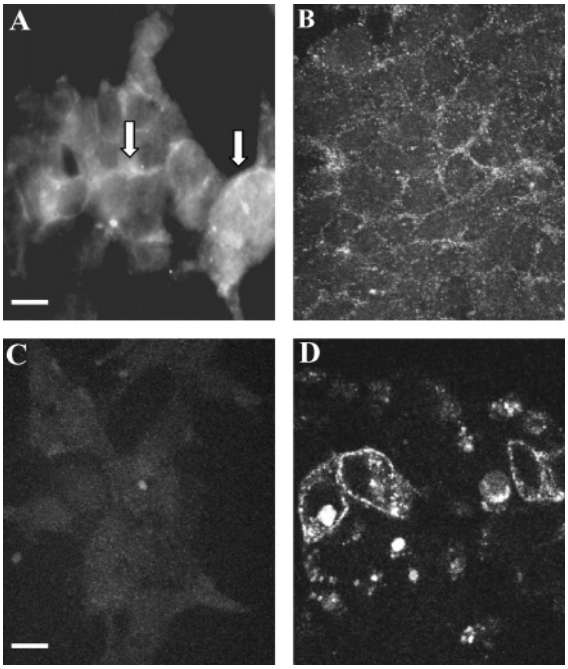

Figure 4. NDP−QD514 targeted hMC4R. (a) HEK293 cells incubated with an MC4R specific antibody after cell fixation and permeabilization showing the distribution of all expressed receptors. Arrows indicate labeling at cell membranes. (b) HEK293 cells incubated with MC4R-specific antibody prior to cell fixation showing the distribution of cell-surface expressed receptors. (c) Live HEK293 cells lacking hMC4R expression, incubated with 10^{-7} M NDP−QD514 15 min prior to imaging. (d) Live cells overexpressing the hMC4R, incubated with 10^{-7} M NDP−QD514. Scale bars = 20 μM.

QD514. The fluorescence values of MT-II−QD514, MT-II−QD595, and Deltorphin-II(Ile−Ile)−QD595 decreased to about one-third those of the bare QDs, but still high enough for bioimaging because of the strong QD photoluminescence.

GPCR Imaging Utilizing QDs. *Targeting hMC4R.* The utility of the EDAC coupling chemistry in generating ligand-modified water-soluble QDs was evaluated. NDP-QD514 was used to target overexpressed melanocortin 4 receptor (MC4R) in HEK293 cells (Figure 4). An MC4R-specific antibody was used to validate receptor expression and determine the cellular distribution of MC4R for comparison with NDP−QD514 mediated imaging. The distribution of total MC4R expression is shown in Figure 4A where cells were permeabilzied then probed with the receptor-specific antibody. This image shows the distribution of all expressed receptor. However, this antibody recognizes an extracellular epitope of the MC4R; therefore, MC4R-transfected HEK293 cells were also incubated with the receptor-specific antibody prior to fixation. Figure 4B shows the distribution of surface-expressed receptor. Control cells without receptor do not show significant fluorescence under either condition (data not shown). Having established that hMC4R was stably expressed, we turned to testing the selectivity of NDP−QD514. HEK293 cells that either did not express (Figure 4c) or expressed hMC4R (Figure 4d) were incubated with NDP−QD514 (10^{-7} M). We clearly observe cell-surface labeling by the NDP−QD514 of the HEK293 cells expressing hMC4R (Figure 4d) with almost no background labeling. These results clearly show that our small ligand labeled water-soluble QDs are easily comparable to commercial fluorescently labeled antibody-based detection methods. Importantly, most receptor antibodies are not raised against extracellular epitopes and therefore do not label only the surface receptors, but rather show the distribution of all receptors (functional or nonfunctional) including those in subcellular compartments such as seen in Figure 4A. Therefore, ligand-conjugated QDs provide an important tool for specifically evaluating the functional receptor complement on the cell surface.

Targeting hDOR. To determine the utility of the APOPA−QDs functionalized with maleimides for conjugation with thiol-bearing ligands, we tested the Deltorphin-II(Ile−Ile)−QD595 targeting to human δ-opioid receptors (hDOR) expressed in CHO cells (Figures 5 and 6). CHO cells with stably expressed receptors were incubated with 0.75 nM Deltorphin-II(Ile−Ile)−QD595 for 1 min, washed, and subsequently imaged (Figure 5). The surface distribution of hDOR can be clearly observed. Since Deltorphin-II(Ile−Ile) is a known agonist, it can activate hDOR and therefore should be internalized. Cells expressing hDOR were incubated for 1 min or 20 min with the Deltorphin-II(Ile−Ile)−QD595. Interestingly, after 1 min we only observed cell-surface labeling, while at 20 min, we can directly observe receptor internalization. As shown in Figure 5, this agonist-mediated activity is retained when the ligand is conjugated on the QD. Control experiments show no cellular labeling or receptor internalization. Thus, these results not only show that the amine-modified QDs are suitable for ligand conjugation and cellular labeling of GPCRs but that they can also be internalized in a receptor-dependent fashion.

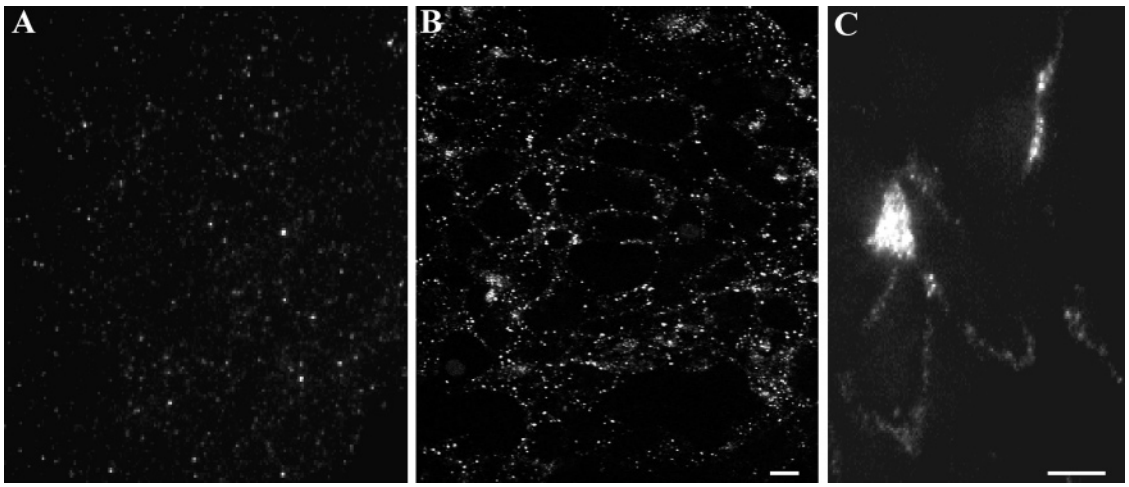

Figure 5. Images of Deltorphin-II(Ile−Ile)−QD595 mediated targeting of human δ-opioid (hDOR) expressed CHO cells. Live cells were incubated for 1 min with 0.75 nM QD−ligand. (a) Cells imaged after 1 min postincubation showing only surface labeling. (b) Cells imaged after incubating for 20 min showing significant organization of Deltorphin-II(Ile−Ile)−QD595 distribution at or near cell surfaces. Scale bars are 10 μm. (c) Image is a magnification showing distribution in four cells, 15 min following the 1 min labeling period.

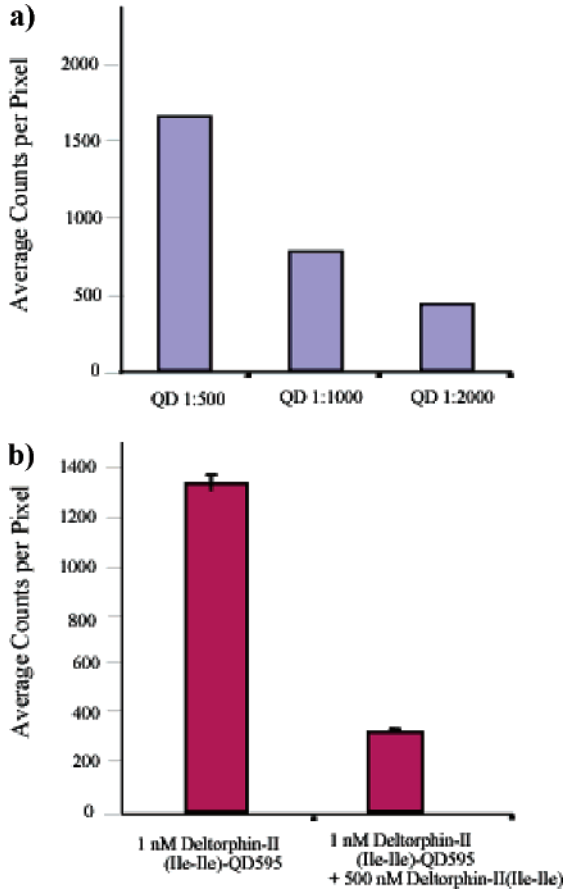

Figure 6. Specificity of Deltorphin-II(Ile−Ile)−QD595 for hDOR on CHO cells. (a) In all experiments, 500 nM of free Deltorphin-II(Ile−Ile) was mixed with varying amounts of Deltorphin-II(Ile−Ile)−QD595 and added to hDOR-expressing CHO cells. (b) Deltorphin-II(Ile−Ile)−QD595 conjugate (1.5 nM) targeting hDOR on CHO cells in the absence and presence of 500 nM of free ligand with prior incubation for 5 min. Measurements are averaged on ten cells per image and five independent images.

In the above experiments, the average number of Deltorphin-II(Ile−Ile)/QD is ∼200; thus, we expected that multivalent interaction (avidity effects) could possibly result in tighter apparent binding constants for Deltorphin-II(Ile−Ile)−QD595 when compared to free Deltorphin-II(Ile−Ile). In a first set of experiments, CHO cells overexpressing hDOR were incubated with 500 nM free Deltorphin-II(Ile−Ile) in the presence of varying concentrations of the Deltorphin-II(Ile−Ile)−QD595. Interestingly, QD−conjugate concentrations in the range 0.375−1.5 nM showed clear cellular labeling, even in the presence of 500 nM of free Deltorphin-II(Ile−Ile) ligands (Figure 6a). These data suggest that the multivalent or avidity effects increase the binding of the labeled QDs which cannot be competed off by the free ligand. In a second experiment, we envisioned that adding free ligand prior to adding QD-conjugated ligand would possibly prevent QD binding. To test this, we added 500 nM of free Deltorphin-II(Ile−Ile) ligand to the cells and incubated for 5 min prior to adding the QD−Deltorphin-(Ile−Ile). The QD−Deltorphin-II(Ile−Ile) was added for 1 min followed by washing the cells and imaging. As expected, incubation of cells with 500 nM of free Deltorphin-II(Ile−Ile) prior to adding the QD−Deltorphin-II(Ile−Ile) prevented significant QD binding as seen by the decrease in the average signal per pixel, from ∼1350 to ∼300 (Figure 6b). The competition experiments taken together establish that the QD conjugates target the hDOR specifically but with a much higher binding constant possibly due to a strong multivalent effect, which may aid in visualizing low copy number receptors. Future experiments will aim to develop approaches for controlling and measuring ligand density on QD surfaces as well as to systematically explore the utility of avidity effects.

Single-Molecule Detection of GPCRs. Single-molecule imaging has emerged as a particularly useful method for investigating receptor localization and trafficking in live cells and in model bilayers (*37*). QDs provide certain advantages over traditional fluorophores due to their broad absorption spectra, tunable emission, and resistance to photobleaching. In order to test the suitability of our ligand-conjugated QDs for single-molecule imaging studies, we chose the human δ-opioid receptor (hDOR) as a target. In these experiments, we directly compare the Deltorphin-II(Ile−Ile)−QD595 conjugate to a Deltorphin-II(Ile−Ile) ligand labeled with Cy3, a widely used fluorophore.

Purified hDOR was incorporated into an artificial lipid bilayer formed on a fused silica coverslip modified by a thin 5-nm-thick polyacrylamide brush. Single-molecule fluorescence was recorded with a total internal reflection fluorescence system, by excitation with an argon ion laser at 488 nm for QDs and 514.5 nm for Cy3. Fluorescence images for hDOR binding for both Deltorphin-II(Ile−Ile)−QD595 and Deltorphin-II(Ile−Ile)−Cy3 were captured as a 500 frame movie, in which the exposure (integration) time was 3 s for each frame. We observed that both Deltorphin-II(Ile−Ile)−QD595 and Deltorphin-II(Ile−Ile)−Cy3 had similar average residence times (bimodal: ∼30 s and hundreds of seconds) on single hDORs (Figure 7). This would at first appear to be in contradiction to the avidity effect observed at cell surfaces; however, in the single-molecule model

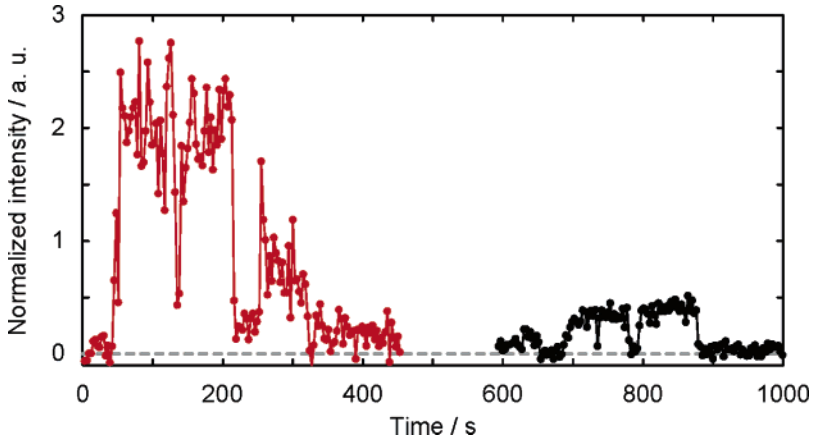

Figure 7. Comparison of fluorescence intensity of Deltorphin-II(Ile−Ile)−QD595 (red) and Deltorphin-II(Ile−Ile)−Cy3 (black) in the presence of hDOR in a lipid bilayer. (Fluorescence intensities after background subtraction.) Fluorescence is normalized at a laser power of 0.05 mW. The one-step increase and decrease indicate one single-molecule event.

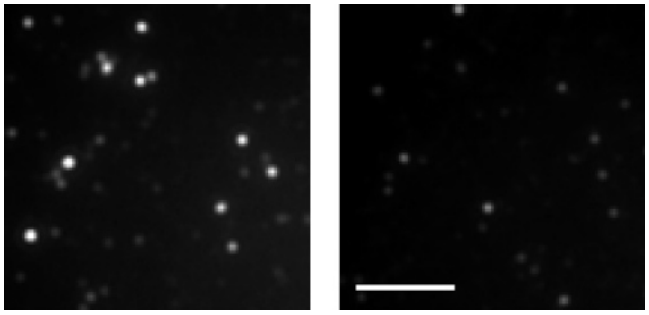

Figure 8. Specific targeting in single-molecule experiments. Cumulative fluorescence images of Deltorphin-II(Ile−Ile)−QD595 (2 nM) bound to hDOR in a lipid bilayer: (a) with and (b) without free Deltorphin-II(D-Ala2) (19 μM). (Same contrast. Image size 16 μm × 16 μm. Scale and illumination are identical in both images, and scale bar is 5 μm.) The 300-frame movies for both (a) and (b) are available online in the Supporting Information.

system, the receptors are at a very low concentration and thus several microns apart, which likely precludes multivalent binding. Most importantly, the fluorescence from QD conjugates was measured to be about sixfold stronger than that from Cy3. This increased fluorescence, combined with other advantages of the QDs such as resistance to photobleaching and multiplexing, provides a potential alternative imaging agent in single-molecule experiments for both model systems and in live cells.

We also considered the possibility that the QD conjugates could possibly bind nonspecifically to the model bilayer. Thus, in order to test the binding specificity, 2 nM of the Deltorphin-II(Ile−Ile)−QD595 conjugate was incubated with hDOR in the absence and presence of excess (19 μM) free Deltorphin-II(D-Ala2) ligand. The cumulative fluorescence images showed that free ligand significantly reduces Deltorphin-II(Ile−Ile)−QD595 from binding the hDOR (Figure 8). Thus, these experiments clearly demonstrate that observed binding is due to specific interaction of Deltorphin-II(Ile−Ile)−QD595 with the immobilized hDOR. Together with the whole-cell experiments, the single-molecule experiments also suggest that careful control experiments, with and without the targeted receptor, must be routinely performed to distinguish between specific versus nonspecific binding for ligand-targeted QDs.

In conclusion, we have developed a convenient method for synthesizing two types of water-soluble QDs with carboxylic acid and amine functionalities. We tested our approach with two different sizes of bare CdSe/ZnS QDs (QD595 and QD514). Both types of polymer-coated QDs displayed excellent solubility, stability, and fluorescence properties in a wide pH regime. We envisioned that the carboxylic acid functionalized QDs can be utilized for directly coupling amine-containing ligands, while the amine-functionalized QDs can be used for conjugating cysteine-containing ligands. Three small peptide ligands were successfully conjugated to our water-soluble QDs in order to target G-protein-coupled receptors (hMCR and hDOR). The ligand-conjugated QDs were shown to be specific for the targeted receptor and could be utilized for fluorescence imaging of receptors in cells as well as in single-molecule experiments in model bilayers. Thus, our methodology provides an expeditious route for constructing new fluorescent bioconjugates that are amenable for multiplexing and may have utility in studying the localization and trafficking of GPCRs in live cells and in single-molecule experiments.

ACKNOWLEDGMENT

We thank the Bio5, University of Arizona, and the NSF (CHE-0548264 and CHE-0433779) for supporting aspects of this research. We thank members of the Ghosh lab for helpful comments. All ligand labeled and unlabeled water-soluble QDs are freely available from the Ghosh lab for research purposes.

Supporting Information Available: Two movies showing single-molecule GPCR binding events in the presence and absence of inhibitors. This material is available free of charge via the Internet at http://pubs.acs.org.

LITERATURE CITED

(1) Michalet, X., Pinaud, F. F., Bentolila, L. A., Tsay, J. M., Doose, S., Li, J. J., Sundaresan, G., Wu, A. M., Gambhir, S. S., and Weiss, S. (2005) Quantum dots for live cells, in vivo imaging, and diagnostics. *Science 307*, 538−544.

(2) Medintz, I. L., Uyeda, H. T., Goldman, E. R., and Mattoussi, H. (2005) Quantum dot bioconjugates for imaging, labelling and sensing. *Nat. Mater. 4*, 435−446.

(3) Green, M. (2004) Semiconductor quantum dots as biological imaging agents. *Angew. Chem., Int. Ed. 43*, 4129−4131.

(4) Smith, A. M., and Nie, S. M. (2004) Chemical analysis and cellular imaging with quantum dots. *Analyst 129*, 672−677.

(5) Wu, A. M., and Senter, P. D. (2005) Arming antibodies: prospects and challenges for immunoconjugates. *Nat. Biotechnol. 23*, 1137−1146.

(6) Goodwin, D. A., and Meares, C. F. (2001) Advances in pretargeting biotechnology. *Biotechnol. Adv. 19*, 435−450.

(7) Chan, W. C. W., and Nie, S. M. (1998) Quantum dot bioconjugates for ultrasensitive nonisotopic detection. *Science 281*, 2016−2018.

(8) Mattoussi, H., Mauro, J. M., Goldman, E. R., Anderson, G. P., Sundar, V. C., Mikulec, F. V., and Bawendi, M. G. (2000) Self-assembly of CdSe-ZnS quantum dot bioconjugates using an engineered recombinant protein. *J. Am. Chem. Soc. 122*, 12142−12150.

(9) Pathak, S., Choi, S. K., Arnheim, N., and Thompson, M. E. (2001) Hydroxylated quantum dots as luminescent probes for in situ hybridization. *J. Am. Chem. Soc. 123*, 4103−4104.

(10) Ding, S. Y., Jones, M., Tucker, M. P., Nedeljkovic, J. M., Wall, J., Simon, M. N., Rumbles, G., and Himmel, M. E. (2003) Quantum dot molecules assembled with genetically engineered proteins. *Nano Lett. 3*, 1581−1585.

(11) Parak, W. J., Gerion, D., Pellegrino, T., Zanchet, D., Micheel, C., Williams, S. C., Boudreau, R., Le Gros, M. A., Larabell, C. A., and Alivisatos, A. P. (2003) Biological applications of colloidal nanocrystals. *Nanotechnology 14*, R15−R27.

(12) Gerion, D., Pinaud, F., Williams, S. C., Parak, W. J., Zanchet, D., Weiss, S., and Alivisatos, A. P. (2001) Synthesis and properties of biocompatible water-soluble silica-coated CdSe/ZnS semiconductor quantum dots. *J. Phys. Chem. B 105*, 8861−8871.

(13) Dubertret, B., Skourides, P., Norris, D. J., Noireaux, V., Brivanlou, A. H., and Libchaber, A. (2002) In vivo imaging of quantum dots encapsulated in phospholipid micelles. *Science 298*, 1759−1762.

(14) Pinaud, F., King, D., Moore, H. P., and Weiss, S. (2004) Bioactivation and cell targeting of semiconductor CdSe/ZnS nanocrystals with phytochelatin-related peptides. *J. Am. Chem. Soc. 126*, 6115−6123.

(15) Gao, X. H., Chan, W. C. W., and Nie, S. M. (2002) Quantum-dot nanocrystals for ultrasensitive biological labeling and multicolor optical encoding. *J. Biomed. Opt. 7*, 532−537.

(16) Wu, X. Y., Liu, H. J., Liu, J. Q., Haley, K. N., Treadway, J. A., Larson, J. P., Ge, N. F., Peale, F., and Bruchez, M. P. (2003) Immunofluorescent labeling of cancer marker Her2 and other cellular targets with semiconductor quantum dots. *Nat. Biotechnol. 21*, 41−46.

(17) Gao, X. H., Cui, Y. Y., Levenson, R. M., Chung, L. W. K., and Nie, S. M. (2004) In vivo cancer targeting and imaging with semiconductor quantum dots. *Nat. Biotechnol. 22*, 969−976.

(18) Howarth, M., Takao, K., Hayashi, Y., and Ting, A. Y. (2005) Targeting quantum dots to surface proteins in living cells with biotin ligase. *Proc. Natl. Acad. Sci. U.S.A. 102*, 7583−7588.

(19) Groc, L., Heine, M., Cognet, L., Brickley, K., Stephenson, F. A., Lounis, B., and Choquet, D. (2004) Differential activity-dependent regulation of the lateral mobilities of AMPA and NMDA receptors. *Nat. Neurosci. 7*, 695−696.

(20) Gomez, N., Winter, J. O., Shieh, F., Saunders, A. E., Korgel, B. A., and Schmidt, C. E. (2005) Challenges in quantum dot-neuron active interfacing. *Talanta 67*, 462−471.
(21) Tomlinson, I. D., Mason, J. N., Blakely, R. D., and Rosenthal, S. J. (2005) Peptide-conjugated quantum dots: imaging the angiotensin type 1 receptor in living cells. *Methods Mol. Biol. 303*, 51−60.
(22) Hines, M. A., and Guyot-Sionnest, P. (1996) Synthesis and characterization of strongly luminescing ZnS-capped CdSe nanocrystals. *J. Phys. Chem. 100*, 468−471.
(23) Kaiser, E., Colescot, R., Bossinge, C., and Cook, P. I. (1970) Color test for detection of free terminal amino groups in solid-phase synthesis of peptides. *Anal. Biochem. 34*, 595.
(24) Rink, H. (1987) Solid-phase synthesis of protected peptide-fragments using a trialkoxy-diphenyl-methylester resin. *Tetrahedron Lett. 28*, 3787−3790.
(25) Grieco, P., Han, G. X., Weinberg, D., MacNeil, T., Van der Ploeg, L. H. T., and Hruby, V. J. (2002) Design and synthesis of highly potent and selective melanotropin analogues of SHU9119 modified at position 6. *Biochem. Biophys. Res. Commun. 292*, 1075−1080.
(26) Hu, M. L. (1994) Measurement of protein thiol-groups and glutathione in plasma. *Methods Enzymol. 233*, 380−385.
(27) Xiao, D. Q., and Wirth, M. J. (2002) Kinetics of surface-initiated atom transfer radical polymerization of acrylamide on silica. *Macromolecules 35*, 2919−2925.
(28) Osborne, V. L., Jones, D. M., and Huck, W. T. S. (2002). Controlled growth of triblock polyelectrolyte brushes. *Chem. Commun.* 1838−1839.
(29) Smith, E. A., Coym, J. W., Cowell, S. M., Tokimoto, T., Hruby, V. J., Yamamura, H. I., and Wirth, M. J. (2005) Lipid bilayers on polyacrylamide brushes for inclusion of membrane proteins. *Langmuir 21*, 9644−9650.
(30) Cremer, P. S., and Boxer, S. G. (1999) Formation and spreading of lipid bilayers on planar glass supports. *J. Phys. Chem. B 103*, 2554−2559.
(31) Alves, I. D., Salamon, Z., Varga, E., Yamamura, H. I., Tollin, G., and Hruby, V. J. (2003) Direct observation of G-protein binding to the human delta-opioid receptor using plasmon-waveguide resonance spectroscopy. *J. Biol. Chem. 278*, 48890−48897.
(32) Marinissen, M. J., and Gutkind, J. S. (2001) G-protein-coupled receptors and signaling networks: emerging paradigms. *Trends Pharmacol. Sci. 22*, 368−376.
(33) Sawyer, T. K., Sanfilippo, P. J., Hruby, V. J., Engel, M. H., Heward, C. B., Burnett, J. B., and Hadley, M. E. (1980) 4-Norleucine, 7-D-phenylalanine-α-melanocyte-stimulating hormone - a highly potent α-melanotropin with ultralong biological-activity. *Proc. Natl. Acad. Sci. U.S.A. 77*, 5754−5758.
(34) Haskellluevano, C., Miwa, H., Dickinson, C., Hruby, V. J., Yamada, T., and Gantz, I. (1994) Binding and camp studies of melanotropin peptides with the cloned human peripheral melanocortin receptor, Hmc1r. *Biochem. Biophys. Res. Commun. 204*, 1137−1142.
(35) Hruby, V. J., Fang, S., Knapp, R., Kazmierski, W., Lui, G. K., and Yamamura, H. I. (1990) Cholecystokinin analogs with high-affinity and selectivity for brain membrane-receptors. *Int. J. Pept. Protein Res. 35*, 566−573.
(36) Sasaki, Y., Ambo, A., and Suzuki, K. (1991) [D-Ala2]Deltorphin-II analogs with high-affinity and selectivity for δ-opioid receptor. *Biochem. Biophys. Res. Commun. 180*, 822−827.
(37) Weiss, S. (1999) Fluorescence spectroscopy of single biomolecules. *Science 283*, 1676−1683.

BC0601929